Incorporation of Plasticity and Damage Into an Orthotropic Three-Dimensional Model with Tabulated Input Suitable for Use in Composite Impact Problems

Robert K. Goldberg and Kelly S. Carney
NASA Glenn Research Center, Cleveland OH
Paul DuBois
George Mason University, Fairfax VA
Canio Hoffarth and Subramaniam Rajan
Arizona State University, Tempe AZ
Gunther Blankenhorn
Livermore Software Technology Corporation, Livermore CA

ABSTRACT

The need for accurate material models to simulate the deformation, damage and failure of polymer matrix composites under impact conditions is becoming critical as these materials are gaining increased usage in the aerospace and automotive industries. While there are several composite material models currently available within commercial transient dynamic finite element codes, several features have been identified as being lacking in the currently available material models that could substantially enhance the predictive capability of the impact simulations. A specific desired feature pertains to the incorporation of both plasticity and damage within the material model. Another desired feature relates to using experimentally based tabulated stress-strain input to define the evolution of plasticity and damage as opposed to specifying discrete input properties (such as modulus and strength) and employing analytical functions to track the response of the material. To begin to address these needs, a combined plasticity and damage model suitable for use with both solid and shell elements is being developed for implementation within the commercial code LS-DYNA. The plasticity model is based on extending the Tsai-Wu composite failure model into a strain-hardening based orthotropic plasticity model with a non-associative flow rule. The evolution of the yield surface is determined based on tabulated stress-strain curves in the various normal and shear directions and is tracked using the effective plastic strain. The effective plastic strain is computed by using the non-associative flow rule in combination with appropriate numerical methods. To compute the evolution of damage, a strain equivalent semi-coupled formulation is used, in which a load in one direction results in a stiffness reduction in multiple coordinate directions. A specific laminated composite is examined to demonstrate the process of characterizing and analyzing the response of a composite using the developed model.

INTRODUCTION

As composite materials are gaining increased use in aircraft components where impact resistance under high energy impact conditions is important (such as the turbine engine fan case), the need for accurate material models to simulate the deformation,

damage and failure response of polymer matrix composites under impact conditions is becoming more critical. Within commercially available transient dynamic finite element code such as LS-DYNA [1], there are several material models currently available for application to the analysis of composites. The available models include relatively simple models such as a derivative of the Chang-Chang model [2], where criteria related to ratios of stresses to failure strengths are used to signify failure, and the composite elastic constants are selectively reduced based on the failure mode. More sophisticated material models incorporated within transient dynamic finite element codes include continuum damage mechanics based models such as the model developed by Matzenmiller, et al [3]. In this approach, the initiation and accumulation of damage is assumed to be the primary driver of any nonlinearity in the composite response. The failure stresses and strains of the material in each of the coordinate directions are specified by the user, the evolution of the damage is computed based on "damage variables", and the nonlinearity of the material stress-strain response is approximated based on the input data and the evolution of the damage. While not necessarily included within commercial codes currently, another approach that has been used to model the strain rate dependent response of a composite is to assume that all of the nonlinearity is due to deformation mechanisms. An example of this approach was developed by Sun and Chen [4], where a quadratic plastic potential function was developed and the plastic strains were computed based on the gradient of the plastic potential function. Stress-strain curves obtained for various fiber orientation angles are used to characterize the coefficients in the plastic potential function based on the values required to collapse the various separate stress-strain curves into a master curve.

While the material models discussed above and other models have been utilized with some level of success in modeling the nonlinear and impact response of polymer composites, there are some areas where the predictive capability can be improved. Most importantly, the existing models often require significant a priori knowledge of the damage and failure in the analyzed structure such that their use as predictive tools can be limited. While these models generally assume that the nonlinear response of the composite is due to either deformation mechanisms (such as plasticity) or damage mechanisms, an improved model should have the capability to simulate the actual material behavior in which the material nonlinearity is due to a combination of both deformation and damage mechanisms. The input to current material models generally consists of point-wise properties (such as a specified failure stress or failure strain) that lead to curve fit approximations to the material stress-strain curves. This type of approach leads either to models with only a few parameters, which provide a crude approximation at best to the actual stress-strain curve, or to models with many parameters which require a large number of complex tests to characterize. An improved approach would be to use tabulated data from a well-defined set of experiments to accurately define the complete stress-strain response of the material. Furthermore, many of the existing models are only suitable for use with two-dimensional shell elements, which cannot capture the through-thickness response, which may be significant in impact applications. Ideally, a fully three-dimensional formulation suitable for use with solid elements would be desireable, along with a shell element formulation.

To begin to address these needs, a multi-institution consortium has been formed to develop and implement a new composite material model within LS-DYNA, which will be implemented as MAT_213. The material model is meant to be a fully generalized

model suitable for use with any composite architecture (unidirectional, laminated or textile). For the deformation model, the commonly used Tsai-Wu composite failure criteria has been generalized and extended to a strain-hardening model with a quadratic yield function and a non-associative flow rule. The coefficients of the yield function for the new composite model are determined based on tabulated stress-strain curves in the various normal and shear directions, along with selected off-axis curves. The non-associative flow rule is used to compute the components of the plastic strain along with the effective plastic strain. The evolution of the yield stresses in the various coordinate directions is tracked based on the current value of the effective plastic strain. For the damage model, a strain equivalent formulation has been developed, which allows the plasticity and damage calculations to be uncoupled, and the plasticity calculations to take place in the effective stress space. In traditional damage mechanics models such as the one developed by Matzenmiller et al [3], a load in a particular coordinate direction is assumed to result in a stiffness reduction only in the direction of the applied load. However, for reasons to be discussed later in this paper, in the current model a semi-coupled formulation is developed in which a load in one direction results in a stiffness reduction in all of the coordinate directions.

In the following sections of this paper, a summary of the derivation of the rate-independent deformation model is presented. The procedures to be used to characterize the material constants in the yield function and the flow law are discussed. Next, the rationale for, and detailed derivation of, the semi-coupled damage model is discussed along with a summary of the test matrix that will be required to properly characterize and validate the developed model. Finally, selected verification studies that have been conducted to ensure that the deformation model has been implemented correctly are presented.

DEFORMATION MODEL DERIVATION

A general quadratic three-dimensional orthotropic yield function based on the Tsai-Wu failure model is specified as follows, where 1, 2, and 3 refer to the principal material directions.

$$
\begin{aligned}
f(\sigma) = a + &\begin{pmatrix} F_1 & F_2 & F_3 & 0 & 0 & 0 \end{pmatrix}
\begin{pmatrix} \sigma_{11} \\ \sigma_{22} \\ \sigma_{33} \\ \sigma_{12} \\ \sigma_{23} \\ \sigma_{31} \end{pmatrix} \\
&+ \begin{pmatrix} \sigma_{11} & \sigma_{22} & \sigma_{33} & \sigma_{12} & \sigma_{23} & \sigma_{31} \end{pmatrix}
\begin{pmatrix}
F_{11} & F_{12} & F_{13} & 0 & 0 & 0 \\
F_{12} & F_{22} & F_{23} & 0 & 0 & 0 \\
F_{13} & F_{23} & F_{33} & 0 & 0 & 0 \\
0 & 0 & 0 & F_{44} & 0 & 0 \\
0 & 0 & 0 & 0 & F_{55} & 0 \\
0 & 0 & 0 & 0 & 0 & F_{66}
\end{pmatrix}
\begin{pmatrix} \sigma_{11} \\ \sigma_{22} \\ \sigma_{33} \\ \sigma_{12} \\ \sigma_{23} \\ \sigma_{31} \end{pmatrix}
\end{aligned}
\tag{1}
$$

In the yield function, σ_{ij} represents the stresses and F_{ij} and F_k are coefficients that vary based on the current values of the yield stresses in the various coordinate directions. By allowing the coefficients to vary, the yield surface evolution and hardening in each of the material directions can be precisely defined. The values of the normal and shear coefficients can be determined by simplifying the yield function for the case of unidirectional tensile and compressive loading in each of the coordinate directions along with shear tests in each of the shear directions, with results as shown below

$$
\begin{aligned}
&a = -1 \\
&F_1 = \frac{1}{\sigma_{11}^T} - \frac{1}{\sigma_{11}^C} \qquad F_{11} = \frac{1}{\sigma_{11}^T \sigma_{11}^C} \qquad F_{44} = \frac{1}{\sigma_{12}^2} \\
&F_2 = \frac{1}{\sigma_{22}^T} - \frac{1}{\sigma_{22}^C} \qquad F_{22} = \frac{1}{\sigma_{22}^T \sigma_{22}^C} \qquad F_{55} = \frac{1}{\sigma_{23}^2} \\
&F_3 = \frac{1}{\sigma_{33}^T} - \frac{1}{\sigma_{33}^C} \qquad F_{33} = \frac{1}{\sigma_{33}^T \sigma_{33}^C} \qquad F_{66} = \frac{1}{\sigma_{31}^2}
\end{aligned}
\tag{2}
$$

In the above equation, the stresses are the current value of the yield stresses in the normal and shear directions (determined using procedures to be discussed below), where the superscript T indicates the tensile yield stress, and the superscript C indicates the absolute value of the compressive yield stress. To determine the values of the off-axis coefficients (which are required to capture the stress interaction effects), the results from 45° off-axis tests in the various coordinate directions can be used. An important point to note is that due to experimental or numerical variability, or alternatively just due to the fundamental behavior of the material, computing the off-diagonal terms of the yield function in this manner may result in a yield function that is not convex (which is a requirement for plasticity theory [5]). As a result, to satisfy the requirements of the chosen yield function, the off-diagonal terms may need to be adjusted based on the values of the other coefficients in the yield function in order to ensure convexity of the yield surface.

A non-associative flow rule is used to compute the evolution of the components of plastic strain. The plastic potential for the flow rule is shown below

$$
h = \sqrt{H_{11}\sigma_{11}^2 + H_{22}\sigma_{22}^2 + H_{33}\sigma_{33}^2 + 2H_{12}\sigma_{11}\sigma_{22} + 2H_{23}\sigma_{22}\sigma_{33} + 2H_{31}\sigma_{33}\sigma_{11} + H_{44}\sigma_{12}^2 + H_{55}\sigma_{23}^2 + H_{66}\sigma_{31}^2} \tag{3}
$$

where σij are the current values of the stresses and H_{ij} are independent coefficients, which are assumed to remain constant. The values of the coefficients are computed based on average plastic Poisson's ratios [6]. The plastic potential function in Equation (3) is used in a flow law to compute the components of the plastic strain rate, where the usual normality hypothesis from classical plasticity [5] is assumed to apply and the variable $\dot{\lambda}$ is a scalar plastic multiplier.

$$
\dot{\boldsymbol{\varepsilon}}^p = \dot{\lambda} \frac{\partial h}{\partial \boldsymbol{\sigma}} \tag{4}
$$

Given the flow law, the principal of the equivalence of plastic work [5] can be used to determine expressions for the effective stress and effective plastic strain. By following this procedure, one can conclude that the plastic potential function h can be

defined as the effective stress and the plastic multiplier can be defined as the effective plastic strain rate.

To compute the current value of the yield stresses needed for the yield function, the common practice in plasticity constitutive equations is to use analytical functions to define the evolution of the stresses as a function of the components of plastic strain (or the effective plastic strain). Alternatively, in the developed model tabulated stress-strain curves are used to track the yield stress evolution. The user is required to input twelve stress versus plastic strain curves. Specifically, the required curves include uniaxial tension curves in each of the normal directions (1,2,3), uniaxial compression curves in each of the normal directions (1,2,3), shear stress-strain curves in each of the shear directions (1-2, 2-3 and 3-1), and 45 degree off-axis tension curves in each of the 1-2, 2-3 and 3-1 planes. The 45 degree curves are required in order to properly capture the stress interaction effects. By utilizing tabulated stress-strain curves to track the evolution of the deformation response, the experimental stress-strain response of the material can be captured exactly without any curve fit approximations. The required stress-strain data can be obtained either from actual experimental test results or by appropriate numerical experiments utilizing stand-alone codes. Currently, only static test data is considered. Future efforts will involve adding strain rate and temperature dependent effects to the computations. To track the evolution of the deformation response along each of the stress-strain curves, the effective plastic strain is chosen to be the tracking parameter. Using a numerical procedure based on the radial return method [5] in combination with an iterative approach, the effective plastic strain is computed for each time/load step. The stresses for each of the tabulated input curves corresponding to the current value of the effective plastic strain are then used to compute the yield function coefficients.

DAMAGE MODEL DERIVATION

The deformation portion of the material model provides the majority of the capability of the model to simulate the nonlinear stress-strain response of the composite. However, in order to capture the nonlinear unloading and local softening of the stress-strain response often observed in composites [7], a complementary damage law is required. In the damage law formulation, strain equivalence is assumed, in which for every time step the total, elastic and plastic strains in the actual and effective stress spaces are the same [8]. The utilization of strain equivalence permits the plasticity and damage calculations to be uncoupled, as all of the plasticity computations can take place in the effective stress space.

The first step in the development of the damage model is to relate the actual stresses to a set of effective stresses by use of a damage tensor **M**

$$\boldsymbol{\sigma} = \mathbf{M}\boldsymbol{\sigma}_{eff} \tag{5}$$

The effective stress rate tensor can be related to the total and plastic strain rate tensors by use of the standard elasto-plastic constitutive equation

$$\dot{\boldsymbol{\sigma}}_{eff} = \mathbf{C}\left(\dot{\boldsymbol{\varepsilon}} - \dot{\boldsymbol{\varepsilon}}_{p}\right) \tag{6}$$

where **C** is the standard elastic stiffness matrix and the actual total and plastic strain rate tensors are used due to the strain equivalence assumption. By differentiating Equation (5) and substituting in Equation (6), the actual stress rate can be written in terms of the total and plastic strain rates and the actual stress. In the following expression, Voigt notation is assumed to be appropriate and the damage tensor is assumed to be invertible.

$$\begin{aligned}\dot{\boldsymbol{\sigma}} &= \mathbf{M}\dot{\boldsymbol{\sigma}}_{eff} + \dot{\mathbf{M}}\boldsymbol{\sigma}_{eff} \\ \dot{\boldsymbol{\sigma}} &= \mathbf{M}\mathbf{C}\left(\dot{\boldsymbol{\varepsilon}} - \dot{\boldsymbol{\varepsilon}}_p\right) + \dot{\mathbf{M}}\mathbf{M}^{-1}\boldsymbol{\sigma}\end{aligned} \tag{7}$$

An algorithm to carry out the uncoupled plasticity/damage analysis is summarized below. In the algorithm, the superscript "n" represents values computed in the previous time step, and the superscript "n+1" indicates values to be computed in the current time step. In the first step of the algorithm, the actual stresses are converted into effective stresses using the damage tensor **M**. In the second step, the plasticity calculations are carried out in the effective stress space to compute the current value of the plastic strain rate, and the effective stress values are updated. Next, in step 3 the damage tensor is modified based on the computed plastic strain rate. Finally, in step 4 the modified damage tensor is used to compute the updated values of the actual stresses based on the updated effective stresses. The algorithm is summarized symbolically below, where Δt is the time step.

$$\begin{aligned}&1.)\ \boldsymbol{\sigma}_{eff}^{n} = \left(\mathbf{M}^{-1}\right)^{n}\boldsymbol{\sigma}^{n} \\ &2.)\ \boldsymbol{\sigma}_{eff}^{n+1} = \boldsymbol{\sigma}_{eff}^{n} + \mathbf{C}\left(\dot{\boldsymbol{\varepsilon}} - \dot{\boldsymbol{\varepsilon}}_p\right)\Delta t \\ &3.)\ \mathbf{M}^{n+1} = \mathbf{M}^{n} + \Delta\mathbf{M}\left[\dot{\boldsymbol{\varepsilon}}_p\right] \\ &4.)\ \boldsymbol{\sigma}^{n+1} = \mathbf{M}^{n+1}\boldsymbol{\sigma}_{eff}^{n+1}\end{aligned} \tag{8}$$

To ensure that the strain equivalence assumption is valid for this approach, the equations utilized in the algorithm should be able to be manipulated to yield an equation similar to that shown in the second expression in Equation (7), which was derived based solely on the strain equivalence assumption. By starting with the equation shown in step 4 of the algorithm, substituting the equation used in step 2 of the algorithm in for the modified effective stress, and breaking up the modified damage tensor into the sum of the current value of the damage tensor and the increment in the damage tensor ($\Delta\mathbf{M}$), the following set of equations is developed.

$$\begin{aligned}\boldsymbol{\sigma}^{n+1} &= \mathbf{M}^{n+1}\left[\left(\mathbf{M}^{-1}\right)^{n}\boldsymbol{\sigma}^{n} + \mathbf{C}\left(\dot{\boldsymbol{\varepsilon}} - \dot{\boldsymbol{\varepsilon}}_p\right)\Delta t\right] \\ \boldsymbol{\sigma}^{n+1} &= \mathbf{M}^{n+1}\mathbf{C}\left(\dot{\boldsymbol{\varepsilon}} - \dot{\boldsymbol{\varepsilon}}_p\right)\Delta t + \mathbf{M}^{n+1}\left(\mathbf{M}^{-1}\right)^{n}\boldsymbol{\sigma}^{n} \\ \boldsymbol{\sigma}^{n+1} &= \left(\mathbf{M}^{n} + \Delta\mathbf{M}\right)\mathbf{C}\left(\dot{\boldsymbol{\varepsilon}} - \dot{\boldsymbol{\varepsilon}}_p\right)\Delta t + \left(\mathbf{M}^{n} + \Delta\mathbf{M}\right)\left(\mathbf{M}^{-1}\right)^{n}\boldsymbol{\sigma}^{n} \\ \boldsymbol{\sigma}^{n+1} &= \mathbf{M}^{n+1}\mathbf{C}\left(\dot{\boldsymbol{\varepsilon}} - \dot{\boldsymbol{\varepsilon}}_p\right)\Delta t + \boldsymbol{\sigma}^{n} + \Delta\mathbf{M}\left(\mathbf{M}^{-1}\right)^{n}\boldsymbol{\sigma}^{n} \\ \frac{\boldsymbol{\sigma}^{n+1} - \boldsymbol{\sigma}^{n}}{\Delta t} &= \mathbf{M}^{n+1}\mathbf{C}\left(\dot{\boldsymbol{\varepsilon}} - \dot{\boldsymbol{\varepsilon}}_p\right) + \frac{\Delta\mathbf{M}}{\Delta t}\left(\mathbf{M}^{-1}\right)^{n}\boldsymbol{\sigma}^{n}\end{aligned} \tag{9}$$

To a first order approximation, the last expression in Equation (9) corresponds to the second expression in Equation (7), which indicates that strain equivalence assumption is appropriate for the combined plasticity/damage algorithm.

Given the usual assumption that the actual stress tensor and the effective stress tensor are symmetric, the actual stresses can be related to the effective stresses in the following manner, where the damage tensor **M** is assumed to have a maximum of 36 independent components.

$$\begin{pmatrix} \sigma_{xx} \\ \sigma_{yy} \\ \sigma_{zz} \\ \sigma_{xy} \\ \sigma_{yz} \\ \sigma_{xz} \end{pmatrix} = [\mathbf{M}] \begin{pmatrix} \sigma_{xx}^{eff} \\ \sigma_{yy}^{eff} \\ \sigma_{zz}^{eff} \\ \sigma_{xy}^{eff} \\ \sigma_{yz}^{eff} \\ \sigma_{xz}^{eff} \end{pmatrix} \tag{10}$$

In many damage mechanics models for composites, for example [3,7], the damage tensor is assumed to be diagonal or manipulated to be a diagonal tensor, leading to the following form.

$$[\mathbf{M}] = \begin{bmatrix} M_{11} & 0 & 0 & 0 & 0 & 0 \\ 0 & M_{22} & 0 & 0 & 0 & 0 \\ 0 & 0 & M_{33} & 0 & 0 & 0 \\ 0 & 0 & 0 & M_{44} & 0 & 0 \\ 0 & 0 & 0 & 0 & M_{55} & 0 \\ 0 & 0 & 0 & 0 & 0 & M_{66} \end{bmatrix} \tag{11}$$

The shear terms M_{44}, M_{55} and M_{66} can be independent (such as in Matzenmiller, et al [3]) or functions of the normal damage terms M_{11}, M_{22} and M_{33}.

The implication of a diagonal damage tensor is that loading the composite in a particular coordinate direction only leads to a stiffness reduction in the direction of the load due to the formation of matrix cracks perpendicular to the direction of the load. However, several recent experimental studies [9, 10, 11] have shown that in actual composites, particularly those with complex fiber architectures, a load in one coordinate direction can lead to stiffness reductions in multiple coordinate directions. One example of this phenomena can be seen in Figure 1, which came from research conducted by Salem and Wilmoth [11]. The figure shows a triaxially braided composite which has been loaded in tension in the transverse direction and then reloaded in compression in the longitudinal direction. As can be seen in the figure, after loading in the transverse direction significant damage above and beyond simple matrix cracks was present in the material. As a result, when the material was reloaded in the longitudinal direction, the measured longitudinal modulus was significantly reduced from the baseline value, indicating that the damage resulting from the transverse load affected the stiffness in the longitudinal direction. There have been limited attempts to incorporate this damage

coupling into an analytical technique, for example by Voyiadjis and Park [12] and Bednarcyk, et al [13]. However, these efforts were developed within the overall concept of a damage mechanics theory in which all of the nonlinearity of the composite response was assumed to be due to damage mechanisms. Furthermore, in the developed theoretical approaches analytical functions were used to track the evolution of the damage and the reduction of the stiffness. The efforts described in the current paper are geared towards developing a damage theory, uncoupled from the plasticity theory, which tracks the stiffness reduction and damage accumulation as a function of the plastic strain by the use of tabulated input.

One approach to incorporating the coupling of damage modes would be to use a non-diagonal damage tensor, such as the one shown below for the case of plane stress.

$$\begin{pmatrix} \sigma_{xx} \\ \sigma_{yy} \\ \sigma_{xy} \end{pmatrix} = \begin{bmatrix} M_{11} & M_{12} & M_{13} \\ M_{21} & M_{22} & M_{23} \\ M_{31} & M_{32} & M_{33} \end{bmatrix} \begin{pmatrix} \sigma_{xx}^{eff} \\ \sigma_{yy}^{eff} \\ \sigma_{xy}^{eff} \end{pmatrix} \tag{12}$$

However, while this formulation would allow for directional coupling, it would have the side effect of a unidirectional load in the actual stress space resulting in a multiaxial load in the effective stress space. For the strain equivalent combined plasticity damage formulation envisioned for this model, this would be an undesirable side effect as the plasticity calculations could be adversely affected due to the introduction of nonphysical stresses.

To avoid the undesired stress coupling, a diagonal damage tensor is required. However, to account for the damage interaction in at least a semi-coupled sense, each term in the diagonal damage matrix should be a function of the plastic strains in each of the normal and shear coordinate directions, as follows for the example of the M_{11} term for the plane stress case

$$M_{11} = M_{11}\left(\varepsilon_{xx}^{p}, \varepsilon_{yy}^{p}, \varepsilon_{xy}^{p}\right) \tag{13}$$

To explain this concept graphically, a schematic is shown in Figure 2 for the case of loading in the x coordinate direction. A plastic strain is applied to an undamaged specimen, with an original area A_{xx} perpendicular to the x axis and an original area A_{yy} perpendicular to the y axis. The undamaged modulus in the x direction is E_{xx} and the undamaged modulus in the y direction is equal to E_{yy}. The specimen is damaged due to the plastic strain. The original specimen is unloaded and reloaded elastically in the x direction. Due to the damage, the reloaded specimen has a reduced area in the x direction of A_{xx}^{dxx} and a reduced modulus in the x direction of E_{xx}^{dxx}. The reduced area and modulus are a function of the damage induced by the plastic strain in the x direction as follows

$$\begin{aligned} E_{xx}^{dxx} &= \left(1 - d_{xx}^{xx}\left(\varepsilon_{xx}^{p}\right)\right)E_{xx} \\ A_{xx}^{dxx} &= \left(1 - d_{xx}^{xx}\left(\varepsilon_{xx}^{p}\right)\right)A_{xx} \end{aligned} \tag{14}$$

where d_{xx}^{xx} is the damage in the x direction due to a load in the x direction. Alternatively, if the damaged specimen was reloaded elastically in the y direction, due to the assumed damage coupling the reloaded specimen would have a reduced area in the y direction of A_{yy}^{dxx} and a reduced modulus in the y direction of E_{yy}^{dxx} due to the load in the x direction. The reduced area and modulus are again a function of the damage induced by the plastic strain in the x direction as follows

$$\begin{aligned} E_{yy}^{dxx} &= \left(1 - d_{xx}^{yy}\left(\varepsilon_{xx}^{p}\right)\right)E_{yy} \\ A_{yy}^{dxx} &= \left(1 - d_{xx}^{yy}\left(\varepsilon_{xx}^{p}\right)\right)A_{yy} \end{aligned} \tag{15}$$

where d_{xx}^{yy} is the damage in the y direction due to a load in the x direction. Similar arguments can be made and equations developed for the situation where the original specimen is loaded plastically in the y direction.

The next issue is how to properly model the damage coupling for the case of multiaxial loading. A simple case for consideration is a composite specimen being simultaneously strained plastically in the x and y directions. One way to approach the problem would be to assume that the loss in area in the x direction due to the straining in the x direction is as follows.

$$A_{xx} - A_{xx}^{dxx} = A_{xx} d_{xx}^{xx} \tag{16}$$

Next, one can assume that the loss in area in the x direction due to the loading in the y direction is as follows

$$A_{xx} - A_{xx}^{dyy} = A_{xx} d_{yy}^{xx} \tag{17}$$

where A_{xx}^{dyy} is the reduced area in the x direction resulting from a load in the y direction and d_{yy}^{xx} is the damage in the x direction resulting from a load in the y direction. The total loss in area in the x direction could be computed by adding together the two separate area losses to obtain a total loss in area.

$$2A_{xx} - A_{xx}^{dxx} - A_{xx}^{dyy} = A_{xx}\left[d_{xx}^{xx} + d_{yy}^{xx}\right] \tag{18}$$

The ratio of the total damaged area to the undamaged area in the x direction can now be computed, which theoretically would lead to the total amount of damage in the x direction in the composite under biaxial loading

$$\frac{A_{xx} - 2A_{xx} + A_{xx}^{dxx} + A_{xx}^{dyy}}{A_{xx}} = \frac{A_{xx} - A_{xx}\left[d_{xx}^{xx} + d_{yy}^{xx}\right]}{A_{xx}} = 1 - d_{xx}^{xx} - d_{yy}^{xx} \tag{19}$$

The relationship between the actual stress and effective stress in the x direction would then be the following.

$$\sigma_{xx} = \left(1 - d_{xx}^{xx}\left(\varepsilon_{xx}^{p}\right) - d_{yy}^{xx}\left(\varepsilon_{yy}^{p}\right)\right)\sigma_{xx}^{eff} \tag{20}$$

The error in this approach is that the assumption is made that the load in the x and y directions are both acting on undamaged areas. In reality, the loads are acting on damaged areas, and just adding to the damaged area. For example, if one loaded the material in the y direction first, the reduced area in the x direction would be equal to A_{xx}^{dyy} and the reduced modulus in the x direction would be equal to E_{xx}^{dyy}. If one would then subsequently load the material in the x direction, the baseline area in the x direction would not equal the original area A_{xx}, but the reduced area A_{xx}^{dyy}. Likewise, the baseline modulus in the x direction would not be equal to the original modulus E_{xx}, but instead the reduced modulus E_{xx}^{dyy}. Therefore, the loading in the x direction would result in the following further reduction in the area and modulus in the x direction.

$$\begin{aligned} E_{xx}^{dxx} &= \left(1 - d_{xx}^{xx}\left(\varepsilon_{xx}^{p}\right)\right)E_{xx}^{dyy} = \left(1 - d_{xx}^{xx}\left(\varepsilon_{xx}^{p}\right)\right)\left(1 - d_{yy}^{xx}\left(\varepsilon_{yy}^{p}\right)\right)E_{xx} \\ A_{xx}^{dxx} &= \left(1 - d_{xx}^{xx}\left(\varepsilon_{xx}^{p}\right)\right)A_{xx}^{dyy} = \left(1 - d_{xx}^{xx}\left(\varepsilon_{xx}^{p}\right)\right)\left(1 - d_{yy}^{xx}\left(\varepsilon_{yy}^{p}\right)\right)A_{xx} \end{aligned} \tag{21}$$

These results suggest that the relation between the actual stress and the effective stress should be based on a multiplicative combination of the damage terms as opposed to an additive combination of the damage terms. For example, for the case of plane stress, the relation between the actual and effective stresses could be expressed as follows

$$\begin{aligned} \sigma_{xx} &= \left(1 - d_{xx}^{xx}\right)\left(1 - d_{yy}^{xx}\right)\left(1 - d_{xy}^{xx}\right)\sigma_{xx}^{eff} \\ \sigma_{yy} &= \left(1 - d_{xx}^{yy}\right)\left(1 - d_{yy}^{yy}\right)\left(1 - d_{xy}^{yy}\right)\sigma_{yy}^{eff} \\ \sigma_{xy} &= \left(1 - d_{xx}^{xy}\right)\left(1 - d_{yy}^{xy}\right)\left(1 - d_{xy}^{xy}\right)\sigma_{xx}^{eff} \end{aligned} \tag{22}$$

where for each of the damage terms the subscript indicates the direction of the load which initiates the particular increment of damage and the superscript indicates the direction in which the damage takes place. Note that for the full three-dimensional case the stress in a particular coordinate direction is a function of the damage due to loading in all of the coordinate directions (x, y, z, xy, xz and yz). By using a polynomial to describe the damage, the coupled terms represent the reduction to the degree of damage resulting from the fact that in a multiaxial loading case the area reductions are combined.

To properly characterize the damage model, an extensive set of test data is required. Due to the tabulated nature of the input, each of the damage parameters (d_{xx}^{xx}, d_{xx}^{yy}, etc.) has to be determined as a function of the plastic strain in a particular coordinate direction (such as ε_{xx}^{p}). For example, to determine the damage terms for the case of loading in the x direction, a composite specimen has to be loaded to a certain plastic strain level in the x direction. The material is then unloaded to a state of zero stress, and then reloaded elastically in each of the coordinate directions to determine the reduced modulus of the material in each of the coordinate directions. Expressions such as those in Equations (14) and (15) can then be used to determine the required damage parameters for the particular value of plastic strain. The process needs to be repeated for multiple values

of plastic strain in the x direction in order to establish the full characterization of the variation of the damage parameters as a function of the plastic strain in the x direction.

VERIFICATION STUDIES FOR DEFORMATION MODEL

A set of verification studies for the deformation portion of the material model were conducted using data for a T800S/3900-2B unidirectional composite [14]. This particular composite is composed of intermediate modulus, high strength fibers embedded within a toughened epoxy matrix. Full details of the verification studies will be provided in a future paper, however a summary is provided here for completeness. An important point to note is that at the current time only the deformation portion of the material model has been implemented numerically within the LS-DYNA computer code, so only deformation analyses will be discussed here. Future efforts will involve implementing and verifying the damage theory described above. However, since the evolution of the parameters in the damage model will be based on the plastic strains, ensuring that the nonlinear deformation response of the composite is being properly simulated by the material model is critical to ensuring that the subsequent characterization and verification of the damage model is correct.

The input data utilized for the verification studies is a combination of actual experimental data obtained by Raju and Acosta [14] and numerical simulations. The numerical simulations were conducted to obtain required stress-strain curves which were not available from the provided experimental data. To conduct the numerical simulations, micromechanics analyses were conducted where the properties of the fiber and matrix were used to simulate the overall response of the composite. The micromechanics analyses were conducted by using a combination of purely analytical simulations conducted using the NASA Glenn developed MAC/GMC code based on the Generalized Method of Cells [15] and finite element models where the fiber and matrix were explicitly simulated. The fiber was assumed be linear elastic with transversely isotropic properties and the matrix was assumed to be isotropic with an elastic-plastic material response. A fiber volume fraction of 0.54 was assumed based on data presented in Bogert, et al [16]. The constituent material properties were chosen to correlate with composite experimental data obtained by Raju and Acosta [14] and Bogert, et al [16]. The elastic modulus and Poisson's ratio of the matrix were chosen to be values representative of epoxy based materials [17]. The fiber longitudinal modulus, transverse modulus and longitudinal Poisson's ratio were chosen such that the composite longitudinal modulus, transverse modulus and longitudinal Poisson's ratio computed by the micromechanics analyses correlated with the values obtained by Bogert, et al [16]. For the fiber transverse Poisson's ratio, a value representative of that utilized for similar carbon fibers [17] was used. The fiber in-plane shear modulus was chosen such that the computed composite in-plane shear modulus correlated to the composite in-plane shear modulus determined by Raju and Acosta [14]. The transverse shear moduli were computed by appropriate assumptions based on the assumed transverse isotropy of the unidirectional material. The yield stress for the matrix was selected such that the computed in-plane shear stress-strain curve for the composite roughly correlated with the experimental stress-strain curve determined by Raju and Acosta [14]. Full details of the numerical experiments and the process used to correlate

the properties for the numerical experiments will be provided in a future paper. The correlated fiber and matrix properties used for the analyses are provided in Table 1.

To conduct the verification studies, finite element models such as the ones shown in Figure 3 for tension and Figure 4 for shear were used. Note that sixty four eight noded solid elements were used for the analyses. For the tension simulations, the nodes on the left hand side of the model were constrained and a constant displacement in the x direction was applied to the nodes on the right face. For the shear simulations, the nodes on the bottom surface were constrained and a displacement in the x direction was applied to the top surface.

Simulated stress-strain curves were computed for a variety of load cases, examples of which are shown in Figure 5 for the case of [0º] tension, Figure 6 for the case of in-plane shear in the x-y plane and Figure 7 for [45º] off-axis tension in the x-y plane. In all of the figures the "Experimental" curves were the curves that were provided as input data for the material model which are based on the actual or numerically generated stress-strain curves, and the "Simulated" curves were the curves computed using the material model. In all cases, the simulated curves correlated very well to the input curves, indicating that the material model was able to accurately represent the nonlinear deformation of the composite in terms of correctly replicating the input data. Future efforts will involve conducting more complex validation analyses which will include analyzing the deformation response of more complex laminated composites as well as simulating the deformation response of a composite under impact conditions.

CONCLUSIONS

A generalized composite model suitable for use in polymer composite impact simulations has been developed. The theory for the rate independent deformation and damage portions of the composite model have been developed and numerical implementation of the deformation model has been completed. The complete composite model will be implemented into the LS-DYNA commercial transient dynamic finite code as MAT 213. For the deformation model, the Tsai-Wu composite failure model has been generalized into an orthotropic yield function with a non-associative flow rule. Tabulated stress-strain data is utilized to track the deformation response of the material, using the effective plastic strain as the tracking variable. A strain equivalent damage model has been developed in which loading the material in a particular coordinate direction can lead to damage in multiple coordinate directions. The actual and effective stresses are related by multiplicative combinations of the various damage variables.

Future efforts will involve generalizing the deformation model to incorporate the ability to simulate the effects of strain rate and temperature on the material response. The damage model will be numerically implemented within the LS-DYNA code. Methods to model failure and element removal will be developed and implemented into LS-DYNA. Extensive additional verification and validation studies will be conducted to verify the accuracy and capability of the overall material model. Overall, when completed the material model when implemented into MAT 213 will provide significant improvements to the state of the art in the modeling of the impact response of polymer composites.

ACKNOWLEDGEMENTS

Authors Hoffarth and Rajan gratefully acknowledge the support of the Federal Aviation Administration through Grant #12-G-001 entitled "Composite Material Model for Impact Analysis", William Emmerling, Technical Monitor.

REFERENCES

1. Hallquist, J. 2013. *LS-DYNA Keyword User's Manual, Version 970*. Livermore Software Technology Corporation, Livermore, CA.
2. Chang, F.-K. and K.-Y. Chang. 1987. "A Progressive Damage Model for Laminated Composites Containing Stress Concentrations," *Journal of Composite Materials*, 21:834-855.
3. Matzenmiller, A., J. Lubliner, and R.L. Taylor. 1995. "A constitutive model for anisotropic damage in fiber-composites," *Mechanics of Materials*, 20:125-152.
4. Sun, C.T., and J.L. Chen. 1989. "A Simple Flow Rule for Characterizing Nonlinear Behavior of Fiber Composites," *Journal of Composite Materials*, 23:1009-1020.
5. Khan, A.S., and S. Huang. 1995. *Continuum Theory of Plasticity*. John Wiley and Sons, New York.
6. Goldberg, R., K. Carney, P. DuBois, C. Hoffarth, J. Harrington, S. Rajan, and G. Blankenhorn. 2014. "Theoretical Development of an Orthotropic Elasto-Plastic Generalized Composite Model," NASA/TM-2014-218347, National Aeronautics and Space Administration, Washington, D.C.
7. Barbero, E.J. 2013. *Finite Element Analysis of Composite Materials Using ABAQUS*. CRC Press, Boca Raton, FL.
8. Lemaitre, J, and R. Desmorat. 2005. *Engineering Damage Mechanics: Ductile, Creep and Brittle Failures*. Springer, Berlin.
9. Ogasawara, O, T. Ishikawa, T. Yokozeki, T. Shiraishi, and N. Watanabe. 2005. "Effect of on-axis tensile loading on shear properties of an orthogonal 3D woven SiC/SiC composite," *Comp. Sci. Technol.*, 65:2541-2549.
10. Salavatian, M., and L.V. Smith. 2014. "The effect of transverse damage on the shear response of fiber reinforced laminates," *Comp. Sci. Technol.*, 95:44-49.
11. Salem, J., and N. Wilmoth, 2015. Personal Communication.
12. Voyiadjis, G.Z., and T. Park. 1995. "Anisotropic Damage of Fiber-Reinforced MMC Using Overall Damage Analysis,", *Journal of Engineering Mechanics*, 121(11):1209-1217.
13. Bednarcyk, B.A., B. Stier, J.-W. Simon, S. Reese, and E. J. Pineda. 2015. "Meso- and micro-scale modeling of damage in plain weave composites,", *Composite Structures*, 121:258-270.
14. Raju, K.S., and J.F. Acosta. 2010. "Crashworthiness of Composite Fuselage Structures—Material Dynamic Properties, Phase I," DOT/FAA/AR-09/8, U.S. Department of Transportation, Federal Aviation Administration, Washington, D.C.
15. Bednarcyk, B.A., and S.M. Arnold. 2002. "MAC/GMC 4.0 User's Manual - Keywords Manual," NASA/TM-2002-212077/VOL2, National Aeronautics and Space Administration, Washington, D.C.
16. Bogert, P.B., A. Satyanarayana, and P.B. Chunchu 2006. "Comparison of Damage Path Predictions for Composite Laminates by Explicit and Standard Finite Element Analysis Tools." *47th AIAA/ASME/ASCE/AHS/ASC Structures, Structural Dynamics, and Materials Conference*, American Institute for Aeronautics and Astronautics, Washington, D.C.
17. Murthy, P.L.N., C.A. Ginty, and J.G. Sanfeliz,. 1993. "Second Generation Integrated Composite Analyzer (ICAN) Computer Code." NASA TP-3290, National Aeronautics and Space Administration, Washington D.C.

Table 1**.** Fiber and Matrix Constitutive Properties Used for Micromechanics Analyses.

Property	Fiber	Matrix
E_{11} (GPa)	275.6	3.45
E_{22} (GPa)	15.5	15.5
ν_{12}	0.20	0.35
ν_{23}	0.25	0.35
G_{12} (GPa)	103.4	1.27
σ_{yield} (MPa)	N/A	137.8

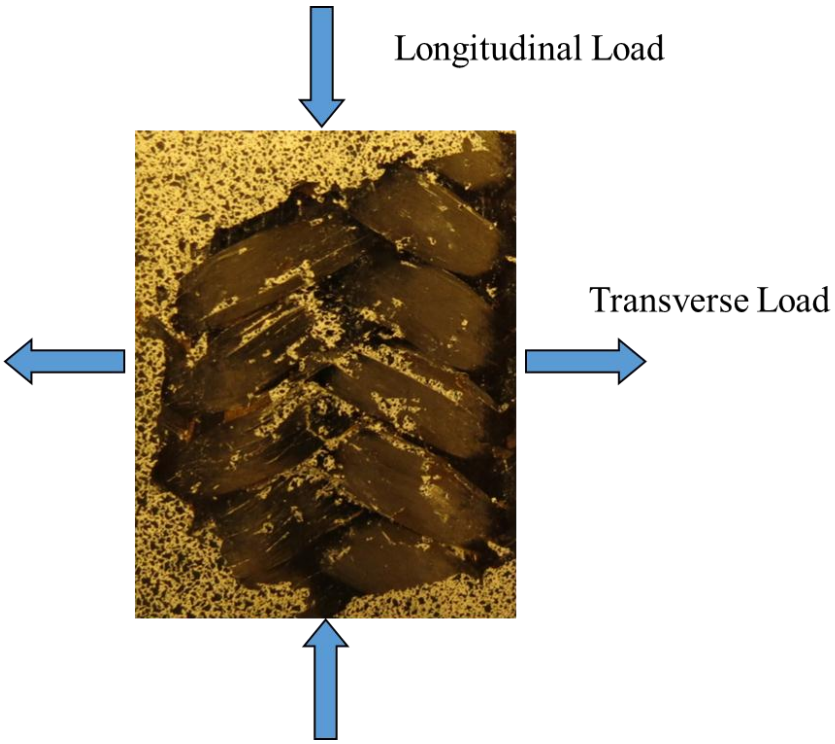

Figure 1. Damage observed in triaxially braided composite subjected to transverse loading followed by longitudinal loading.

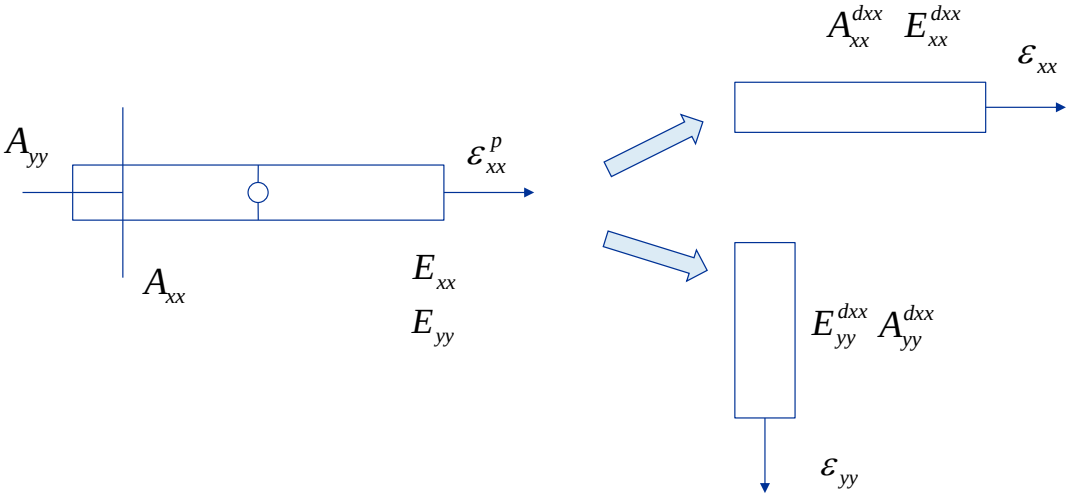

Figure 2. Coupled damage resulting from loading in x coordinate direction.

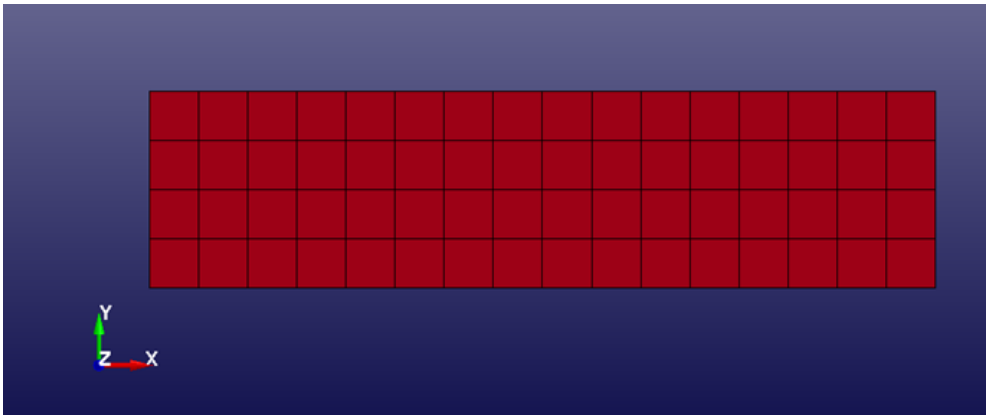

Figure 3. Finite element model for tension verification analyses.

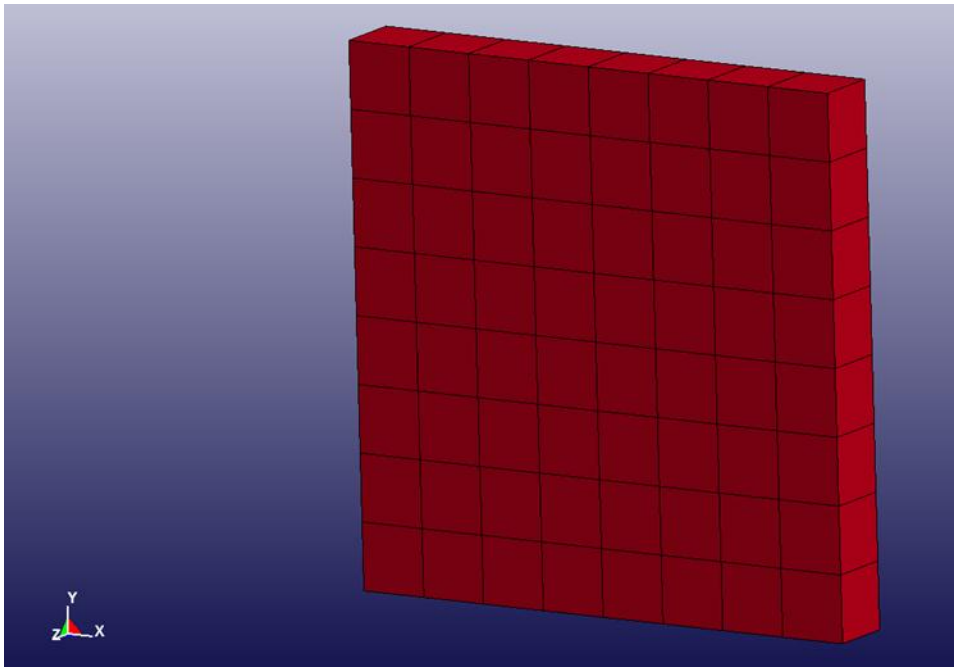

Figure 4. Finite element model for shear verification analyses.

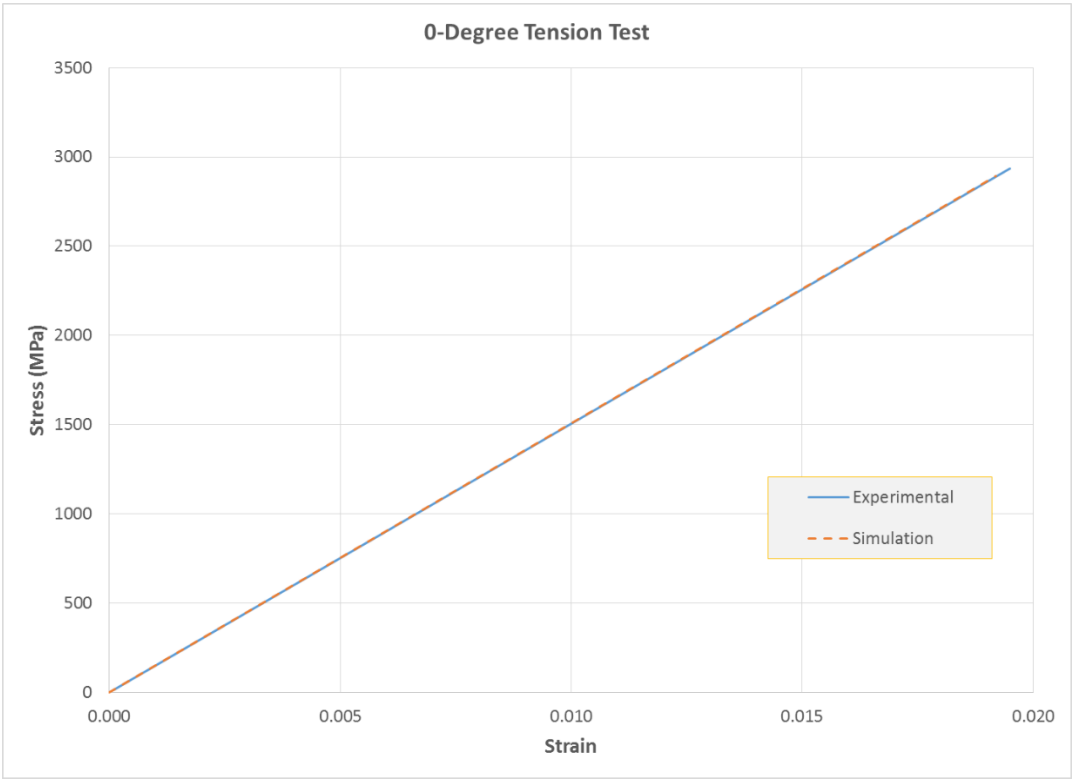

Figure 5. Verification analyses for 0 degree tension test.

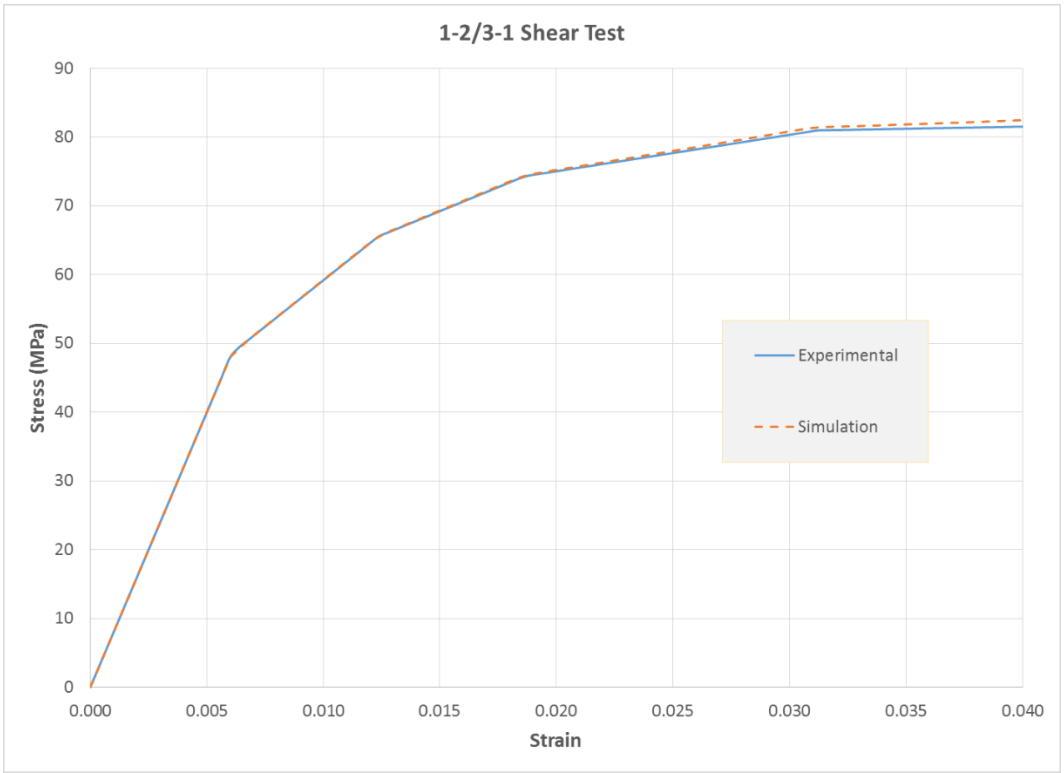

Figure 6: Verification analyses for in-plane shear test.

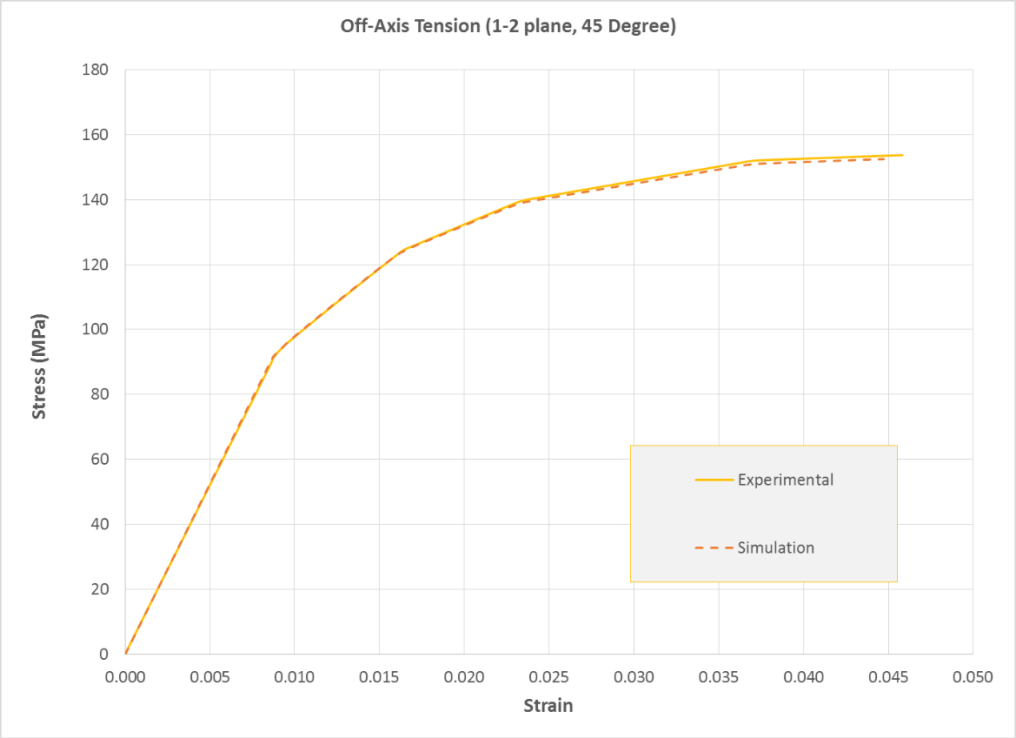

Figure 7. Verification Analyses for 45 degree off-axis tension test.